Gain spectrum of a laser-driven tripod-type atom dynamically induced in the presence of spontaneously generated coherence

Si-Cong Tian,[1] Ren-Gang Wan,[2] Zhi-Hui Kang,[1] Hang Zhang,[3] Yun Jiang,[1] Hai-Ning Cui,[1] and Jin-Yue Gao[1,*]

[1]*Key Lab of Coherent Light and Atomic and Molecular Spectroscopy of Ministry of Education, College of Physics, Jilin University, Changchun 130023, China*
[2]*State Key Laboratory of Transient Optics and Photonics, Xi'an Institute of Optics and Precision Mechanics, Chinese Academy of Sciences, Xi'an 710119, China*
[3]*Changchun Institute of Optics, Fine Mechanics and Physics, Chinese Academy of Sciences, Changchun 130023, China*
**Corresponding author: jygao@mail.jlu.edu.cn*

Received September 15, 2011; revised December 9, 2011; accepted December 11, 2011; posted December 14, 2011 (Doc. ID 154703); published April 4, 2012

We examine the absorption of a weak probe beam in a laser-driven tripod-type atom with three closely lying ground levels, where both the driving and probe lasers interact simultaneously with the three transitions. The effects of spontaneously generated coherence (SGC) are taken into account. We introduce dipole moments in the dressed-state picture and the Hamiltonian in terms of the dressed states describing the interaction between the probe and the atom. Gain spectrum under various conditions are presented and analyzed. We show that the spectral structure and the gain amplitude of the probe are strongly influenced by the effect of SGC and the frequency separation of the three closely lying ground levels. The tripod-type atomic system with quantum interference in spontaneous emission can be simulated in the dressed-state picture of a coherently driven four-level N-type system where no SGC effect exists.

OCIS codes: 270.1670, 270.6620.

1. INTRODUCTION

The coherence generated by the process of spontaneous emission is named spontaneously generated coherence (SGC), which has been intensively studied in recent years. SGC gives rise to a variety of novel quantum effects, such as coherent population trapping [1] and transfer [2], transparency of a short laser pulse [3,4], slowing down of the light pulses [5,6], two-photon correlation [7], photonic band-gap structure [8], quantum interference enhancement with left-handed materials [9], and plasmon-induced enhancement of quantum interference near metallic nanostructures [10].

However, it is very difficult to find a real atomic system with SGC to experimentally demonstrate these phenomena, because SGC exists only in such atoms that have two or more close-lying levels subject to the conditions that these levels are near degenerate and the corresponding dipole matrix elements are nonorthogonal. To observe the phenomena based on SGC in atomic systems without these rigorous conditions, a few methods have been proposed to simulate this intriguing effect. Agarwal has suggested working in such situations where the vacuum of the electromagnetic field is anisotropic [11]. Ficek and Swain showed the simulation of SGC with the coupling of a DC field [12]. SGC has also been studied in dressed states of a laser field [13,14] and a microwave field [15,16]. And Li *et al* suggested an experiment to test the effect of quantum interference because of energy shifts on the emission spectrum [17]. Most recently, we reported experimental investigations of the absorption features in a four-level system with SGC [18–20], which means we can simulate SGC by applying laser fields and the frequency separation can be controlled by the applied fields.

The absorption affected by quantum interference is adequately covered by the three-level V and Λ system. The absorption properties of the V system in the absence of any pump field have been investigated [21], and the existence of quantum interference may lead to amplification without inversion and reverse-saturated absorption. In addition, this system driven by a single coherent field has been studied by Menon and Agarwal [22] under the condition that the coherent field drives only one transition and a probe detects another transition. Later, Dong and Tang [23] have studied the absorption of a weak probe beam by a laser-driven V-type atom with a pair of closely lying excited levels, where both the driving and probe lasers interact simultaneously with the two transitions.

There are also investigations on the Λ-type configuration. Menon and Agarwal investigated the effects of SGC on a standard Λ system driven by two coherent fields under the condition that one field drives only one transition, and they found that the SGC brings about quantitative changes in line profiles of absorption and dispersion [24]. In a later paper [25], the same system with or without an incoherent pump was investigated, where the transient gain properties can be dramatically affected by SGC. And by changing the relative phase between the two fields, the inversionless gain can be modulated in the same system with an incoherent pump [26]. The gain spectrum of a coherently driven Λ-type atom with a pair of closely lying ground levels was examined by Xu and Gao

[27], where a single laser field drives both transitions from the upper state to the lower states simultaneously.

In most of the preceding studies, one usually considered the typical situation that a strong coherent field drives only one transition and a weak probe field detects on a different transition; besides, the SGC effect exists only in atoms that have only two close-lying levels. In this paper we consider a four-level tripod atomic scheme with three closely lying ground levels. The weak probe absorption in the tripod-type atom is investigated under the condition that both the driving field and the probe field interact simultaneously with three different arms. Both degenerate and nondegenerate systems are considered with or without the presence of quantum interference among decay channels. With the help of SGC, we can obtain more gain (or absorption) peaks by only one coupling field, and the spectral structure and the gain amplitude of the probe can be controlled by the SGC effect and the frequency separation of the three closely lying ground levels. This tripod-type atom can be attained in a four-level N-type system [20] in a real atomic system with the help of two coupling fields. Thus it is possible to demonstrate various effects of SGC and show the dependence of level separation on external field experimentally.

The paper is organized as follows. In Section 2, we describe the model and the basic density-matrix equations. By utilizing the quantum-regression theorem, we can obtain the steady-state probe absorption spectrum. In Section 3, we introduce the dipole moments in the dressed-state representation and the Hamiltonian in terms of the dressed states describing the interaction between the probe and the atom. In Section 4 we give the numerical results and analyze the results in the dressed-state representation. In Section 5 we discuss a possible experiment to attain the tripod-type atom with SGC. Finally, in Section 6 we give a summary of the paper.

2. ATOMIC MODEL AND SOLUTION FOR THE ABSORPTION

We consider a four-level atom as shown in Fig. 1. It has three ground levels $|2\rangle$, $|3\rangle$, and $|4\rangle$ and is separated in frequency by ω_{23} and ω_{34}, respectively. The excited level $|1\rangle$ decays to the three lower levels with rates γ_{12}, γ_{13}, and γ_{14}, respectively. The decoherence rates between the ground levels attributable to the collisional relaxation are γ_{23}, γ_{24}, and γ_{34}. The transitions $|1\rangle\leftrightarrow|2\rangle$, $|1\rangle\leftrightarrow|3\rangle$, and $|1\rangle\leftrightarrow|4\rangle$ are simultaneously driven by a laser field of frequency ω_c with Rabi frequencies $\Omega_2 = E_c\mathbf{e}_c\cdot\boldsymbol{\mu}_{12}/2\hbar$, $\Omega_3 = E_c\mathbf{e}_c\cdot\boldsymbol{\mu}_{13}/2\hbar$, and $\Omega_4 = E_c\mathbf{e}_c\cdot\boldsymbol{\mu}_{14}/2\hbar$, where E_c and $\mathbf{e}_c$ are the amplitude and the polarization vector of the driving field and $\boldsymbol{\mu}_{12}$, $\boldsymbol{\mu}_{13}$, and $\boldsymbol{\mu}_{14}$ are the dipole moments of the respective transitions.

It is well known that the quantum interference in the spontaneous emission or the so-called SGC effect is very sensitive to the orientations of the atomic dipole polarizations. The degree of this kind of interference is measured by $p_{ij} = \cos\theta_{ij} (i,j = 2,3,4, i \neq j)$, where θ_{ij} denotes the angle between the two transition dipole moments $\boldsymbol{\mu}_{1i}$ and $\boldsymbol{\mu}_{1j}$. If $\boldsymbol{\mu}_{1i}$ and $\boldsymbol{\mu}_{1j}$ are parallel to each other, then $p_{ij} = 1$ ($\theta_{ij} = 0$) and the interference is maximum, while if $\boldsymbol{\mu}_{1i}$ and $\boldsymbol{\mu}_{1j}$ are perpendicular to each other, then $p_{ij} = 0$ ($\theta_{ij} = 90°$) and the quantum interference disappears.

For simplicity, we assume the dipoles of the excited state to ground states to be equal in magnitude and the angles between each other are the same as well. Then we have $|\boldsymbol{\mu}_{12}| = |\boldsymbol{\mu}_{13}| = |\boldsymbol{\mu}_{14}|$, $\gamma_{12} = \gamma_{13} = \gamma_{14} \equiv \gamma$, and $p_{23} = p_{24} = p_{34} \equiv p$. We further assume that the driving and the probe fields are along the same direction (i.e., $\mathbf{e}_c \| \mathbf{e}_p$), and the angles between $\mathbf{e}_c$ and each of the dipoles are equal, as shown in Fig. 1(b). Thus we have $\Omega_2 = \Omega_3 = \Omega_4 \equiv \Omega$. In the following calculations and discussions, we consider only the case that the three ground levels are equispaced ($\omega_{23} = \omega_{34} \equiv \omega$) and the driven laser is resonant with transition $|1\rangle\leftrightarrow|3\rangle$ ($\Delta_c = 0$). Moreover, we assume $\gamma_{23} = \gamma_{24} = \gamma_{34} \equiv \gamma'$.

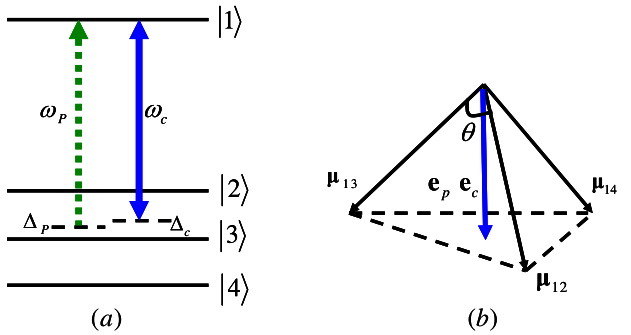

Fig. 1. (Color online) (a) Tripod-type atomic system under consideration. (b) Arrangement of field polarization and dipole moments. θ is the angle between every two dipole moments. The polarization directions of both the driving and the probe fields are the same direction. And the angle between this orientation and each of the dipole moment is the same.

The Hamiltonian describing the interaction between the atom and the driving laser takes the form

$$H_c = -\omega|2\rangle\langle 2| + \omega|4\rangle\langle 4| + \Omega(|1\rangle\langle 2| + |1\rangle\langle 3| + |1\rangle\langle 4| + \text{H.c.}). \quad (1)$$

The time evolution of the density-matrix elements can be derived as follows:

$$\dot{\rho}_{22} = i\Omega(\rho_{12} - \rho_{21}) + \gamma\rho_{11} + \gamma'(\rho_{33} - \rho_{22}) + \gamma'(\rho_{44} - \rho_{22}), \quad (2a)$$

$$\dot{\rho}_{33} = i\Omega(\rho_{13} - \rho_{31}) + \gamma\rho_{11} + \gamma'(\rho_{22} - \rho_{33}) + \gamma'(\rho_{44} - \rho_{33}), \quad (2b)$$

$$\dot{\rho}_{44} = i\Omega(\rho_{14} - \rho_{41}) + \gamma\rho_{11} + \gamma'(\rho_{22} - \rho_{44}) + \gamma'(\rho_{33} - \rho_{44}), \quad (2c)$$

$$\dot{\rho}_{12} = -i\Omega(\rho_{11} - \rho_{22}) + i\Omega(\rho_{32} + \rho_{42}) - (3\gamma/2 + i\omega)\rho_{12}, \quad (2d)$$

$$\dot{\rho}_{13} = -i\Omega(\rho_{11} - \rho_{33}) + i\Omega(\rho_{23} + \rho_{43}) - 3\gamma\rho_{13}/2, \quad (2e)$$

$$\dot{\rho}_{14} = -i\Omega(\rho_{11} - \rho_{44}) + i\Omega(\rho_{24} + \rho_{34}) - (3\gamma/2 - i\omega)\rho_{14}, \quad (2f)$$

$$\dot{\rho}_{23} = i\Omega(\rho_{13} - \rho_{21}) - (i\omega + \gamma')\rho_{23} + p\gamma\rho_{11}, \quad (2g)$$

$$\dot{\rho}_{24} = i\Omega(\rho_{14} - \rho_{21}) - (2i\omega + \gamma')\rho_{24} + p\gamma\rho_{11}, \quad (2h)$$

$$\dot{\rho}_{34} = i\Omega(\rho_{14} - \rho_{31}) - (-i\omega + \gamma')\rho_{34} + p\gamma\rho_{11}, \quad (2i)$$

$$\rho_{11} + \rho_{22} + \rho_{33} + \rho_{44} = 1, \quad (2j)$$

$$\rho_{ij} = \rho_{ij}^*. \quad (2k)$$

Then we suppose a weak probe laser with frequency ω_p scanning over the system. We properly arrange the polarization directions of both the probe and the driving fields so they are along the same direction as shown in Fig. 1(b). The probe field acts on all transitions $|1\rangle\leftrightarrow|2\rangle$, $|1\rangle\leftrightarrow|3\rangle$, and $|1\rangle\leftrightarrow|4\rangle$ simultaneously. The steady-state absorption spectrum $A(\Delta_p)$ is proportional to the Fourier transform of the stationary average value of the two-time commutator of the atomic dipole operators

$$A(\Delta_p) = -\mathrm{Re}\int_0^\infty \lim_{t\to\infty}\langle[P(t+\tau), P^+(t)]\rangle \exp(i\Delta_p\tau)\mathrm{d}\tau, \quad (3)$$

where Δ_p is the detuning of the probe field from the optical transition $|1\rangle\leftrightarrow|3\rangle$. And $P(t) = \mu_{12}|2\rangle\langle 1| + \mu_{13}|3\rangle\langle 1| + \mu_{14}|4\rangle\langle 1|$ is the component of the atomic polarization operator in the direction of the probe polarization, and $\mu_{1i} = \boldsymbol{\mu}_{1i}\cdot\mathbf{e}_p$ $(i = 2, 3, 4)$. With the preceding assumption that the angles between $\mathbf{e}_p$ and each of the dipoles are equal, we have $\mu_{12} = \mu_{13} = \mu_{14} \equiv \mu$.

To evaluate the absorption spectra, we write the density-matrix equations in the form

$$\frac{d}{dt}\psi = L\psi + I, \quad (4)$$

where ψ is a column vector,

$$\psi = (\rho_{12},\rho_{13},\rho_{14},\rho_{21},\rho_{22},\rho_{23},\rho_{24},\rho_{31},\rho_{32},\rho_{33},\rho_{34},\rho_{41},\rho_{42},\rho_{43},\rho_{44},)^T. \quad (5)$$

The matrix I can be written as

$$I = (-i\Omega,-i\Omega,-i\Omega,i\Omega,\gamma,p\gamma,p\gamma,i\Omega,p\gamma,\gamma,p\gamma,i\Omega,p\gamma,p\gamma,\gamma)^T. \quad (6)$$

And L is a time-independent 15×15 matrix whose explicit expression can easily be derived from Eq. (2).

By utilizing the quantum-regression theory [28,29], the steady-state probe absorption spectrum is obtained by using the quantum-regression theorem. The result is

$$\begin{aligned}
A(\Delta_P) = \mu^2\,\mathrm{Re}\{&[M_{11}(\rho_{11}-\rho_{22}) + M_{15}\rho_{21} + M_{19}\rho_{31} + M_{113}\rho_{41} - M_{12}\rho_{23} - M_{13}\rho_{24}]\\
&+ p[M_{12}(\rho_{11}-\rho_{33}) + M_{16}\rho_{21} + M_{110}\rho_{31} + M_{114}\rho_{41} - M_{11}\rho_{32} - M_{13}\rho_{34}]\\
&+ p[M_{13}(\rho_{11}-\rho_{44}) + M_{17}\rho_{21} + M_{111}\rho_{31} + M_{115}\rho_{41} - M_{11}\rho_{42} - M_{12}\rho_{43}]\\
&+ [M_{22}(\rho_{11}-\rho_{33}) + M_{26}\rho_{21} + M_{210}\rho_{31} + M_{214}\rho_{41} - M_{21}\rho_{32} - M_{23}\rho_{34}]\\
&+ p[M_{21}(\rho_{11}-\rho_{22}) + M_{25}\rho_{21} + M_{29}\rho_{31} + M_{213}\rho_{41} - M_{22}\rho_{23} - M_{23}\rho_{24}]\\
&+ p[M_{23}(\rho_{11}-\rho_{44}) + M_{27}\rho_{21} + M_{211}\rho_{31} + M_{215}\rho_{41} - M_{21}\rho_{42} - M_{22}\rho_{43}]\\
&+ [M_{33}(\rho_{11}-\rho_{44}) + M_{37}\rho_{21} + M_{311}\rho_{31} + M_{315}\rho_{41} - M_{31}\rho_{42} - M_{32}\rho_{43}]\\
&+ p[M_{31}(\rho_{11}-\rho_{22}) + M_{35}\rho_{21} + M_{39}\rho_{31} + M_{313}\rho_{41} - M_{32}\rho_{23} - M_{33}\rho_{24}]\\
&+ p[M_{32}(\rho_{11}-\rho_{33}) + M_{36}\rho_{21} + M_{210}\rho_{31} + M_{214}\rho_{41} - M_{31}\rho_{32} - M_{33}\rho_{34}]\},
\end{aligned} \quad (7)$$

where $M_{ij} = [(z-L)^{-1}|_{z=i\Delta_p}]_{ij}$, and $\rho_{ij}|_{i,j=1\to 15}$ are the steady-state $(t\to\infty)$ solutions of Eq. (4).

Equation (7) is the basic result for the discussions to follow, and the gain spectra presented in Section 4 is obtained from Eq. (7).

3. DRESSED-ATOM MODEL

In this section we introduce atomic dipole moments in the dressed-state representation as our basis for the analysis in Section 4. Under the preceding conditions, the four eigenstates can be written in terms of the bare states as

$$|\Psi_i, N\rangle = C_{i1}|1, N-1\rangle + C_{i2}|2, N\rangle + C_{i3}|3, N\rangle + C_{i4}|4, N\rangle \quad (i = 1,2,3,4). \quad (8)$$

In this situation, the coefficients C_{ij} in Eq. (8) are

$$C_{i1} = \frac{\lambda_i(\lambda_i+\omega)(\lambda_i-\omega)}{D_i}, \quad (9a)$$

$$C_{i2} = \frac{\lambda_i(\lambda i-\omega)\Omega}{D_i}, \quad (9b)$$

$$C_{i3} = \frac{(\lambda_i+\omega)(\lambda_i-\omega)\Omega}{D_i}, \quad (9c)$$

$$C_{i4} = \frac{\lambda_i(\lambda_i+\omega)\Omega}{D_i}, \quad (9d)$$

where

$$D_i = \sqrt{\lambda_i^2(\lambda_i-\omega)^2(\lambda_i+\omega)^2 + \Omega^2[\lambda_i^2(\lambda_i-\omega)^2 + (\lambda_i+\omega)^2(\lambda_i-\omega)^2 + \lambda_i^2(\lambda_i+\omega)^2]}. \tag{10}$$

The corresponding eigenvalues λ_i are $\lambda_4 = -\lambda_1 = \sqrt{\kappa_+}$ and $\lambda_3 = -\lambda_2 = \sqrt{\kappa_-}$, where

$$\kappa_\pm = \frac{1}{2}\left[(3\Omega^2+\omega^2) \pm \sqrt{(3\Omega^2+\omega^2)^2 - 4\omega^2\Omega^2}\right]. \tag{11}$$

The matrix elements of the atomic dipole moment in the dressed-state picture take the following form:

$$\langle \Psi_i, N+1|\boldsymbol{\mu}|\Psi_j, N\rangle = C_{i1}^* C_{j2}\boldsymbol{\mu}_{12} + C_{i1}^* C_{j3}\boldsymbol{\mu}_{13} + C_{i1}^* C_{j4}\boldsymbol{\mu}_{14}. \tag{12}$$

It is noted that the interaction of the atom with the vacuum field allows spontaneous emission to occur from states $|\Psi_i, N+1\rangle$ and $|\Psi_j, N\rangle$ only if $\langle \Psi_i, N+1|\boldsymbol{\mu}|\Psi_j, N\rangle \neq 0$ [23].

Under the conditions of $\mu_{12} = \mu_{13} = \mu_{14} \equiv \mu$, the interaction Hamiltonian of the probe beam with the atom is

$$\begin{aligned} H_p &= \frac{1}{2}\mu E_p[e^{-i\omega_p t}(|1\rangle\langle 2| + |1\rangle\langle 3| + |1\rangle\langle 4|) + \text{H.c.}] \\ &= \frac{1}{2}\mu E_p\left(e^{-i\omega_p t}\sum_{i=1}^{4} C_{i1}|\Psi_i\rangle \sum_{j=1}^{4}\sum_{k=2}^{4} C_{jk}^*\langle \Psi_j| + \text{H.c.}\right). \end{aligned} \tag{13}$$

Equation (13) indicates which of the transitions can be coupled by the probe field. Besides, it is noted that the polarization direction of the probe determines the transitions that can be detected. Different transitions can be probed with different weights as the polarization direction changes.

In the next section we present the gain spectra of the probe field under various conditions and analyze them by employing the atomic dipole moments in the dressed-state representation.

4. RESULTS AND ANALYSIS

A. Case of the Degenerate Levels

We first consider the case of the degenerate ground levels where $\omega = 0$. In this case, the eigenvalues are $\lambda_1 = -\sqrt{3}\Omega$, $\lambda_2 = \lambda_3 = 0$, and $\lambda_4 = \sqrt{3}\Omega$, and Eq. (8) can be simplified as

$$|\Psi_1, N\rangle = \frac{1}{\sqrt{6}}\left(\sqrt{3}|1, N-1\rangle + |2, N\rangle + |3, N\rangle + |4, N\rangle\right), \tag{14a}$$

$$|\Psi_2, N\rangle = \frac{1}{\sqrt{12}}\left[\left(-\sqrt{3}-1\right)|2, N\rangle + 2|3, N\rangle + \left(\sqrt{3}-1\right)|4, N\rangle\right], \tag{14b}$$

$$|\Psi_2, N\rangle = \frac{1}{\sqrt{12}}\left[\left(\sqrt{3}-1\right)|2, N\rangle + 2|3, N\rangle + \left(-\sqrt{3}-1\right)|4, N\rangle\right], \tag{14c}$$

$$|\Psi_4, N\rangle = \frac{1}{\sqrt{6}}\left(-\sqrt{3}|1, N-1\rangle + |2, N\rangle + |3, N\rangle + |4, N\rangle\right). \tag{14d}$$

Thus, the atomic dipole moment expressed by Eq. (12) has the following matrix elements:

$$\langle \Psi_1, N+1|\boldsymbol{\mu}|\Psi_1, N\rangle = \frac{\sqrt{3}}{6}(\boldsymbol{\mu}_{12} + \boldsymbol{\mu}_{13} + \boldsymbol{\mu}_{14}), \tag{15a}$$

$$\langle \Psi_1, N+1|\boldsymbol{\mu}|\Psi_2, N\rangle = \frac{\sqrt{6}}{12}\left[\left(1+\sqrt{3}\right)(\boldsymbol{\mu}_{13} - \boldsymbol{\mu}_{12}) + \left(1-\sqrt{3}\right)(\boldsymbol{\mu}_{13} - \boldsymbol{\mu}_{14})\right], \tag{15b}$$

$$\langle \Psi_1, N+1|\boldsymbol{\mu}|\Psi_3, N\rangle = \frac{\sqrt{6}}{12}\left[\left(1-\sqrt{3}\right)(\boldsymbol{\mu}_{13} - \boldsymbol{\mu}_{12}) + \left(1+\sqrt{3}\right)(\boldsymbol{\mu}_{13} - \boldsymbol{\mu}_{14})\right], \tag{15c}$$

$$\langle \Psi_1, N+1|\boldsymbol{\mu}|\Psi_4, N\rangle = \frac{\sqrt{3}}{6}(\boldsymbol{\mu}_{12} + \boldsymbol{\mu}_{13} + \boldsymbol{\mu}_{14}), \tag{15d}$$

$$\langle \Psi_4, N+1|\boldsymbol{\mu}|\Psi_1, N\rangle = -\frac{\sqrt{3}}{6}(\boldsymbol{\mu}_{12} + \boldsymbol{\mu}_{13} + \boldsymbol{\mu}_{14}), \tag{15e}$$

$$\langle \Psi_4, N+1|\boldsymbol{\mu}|\Psi_2, N\rangle = -\frac{\sqrt{6}}{12}\left[\left(1+\sqrt{3}\right)(\boldsymbol{\mu}_{13} - \boldsymbol{\mu}_{12}) + \left(1-\sqrt{3}\right)(\boldsymbol{\mu}_{13} - \boldsymbol{\mu}_{14})\right], \tag{15f}$$

$$\langle \Psi_4, N+1|\boldsymbol{\mu}|\Psi_3, N\rangle = -\frac{\sqrt{6}}{12}\left[\left(1+\sqrt{3}\right)(\boldsymbol{\mu}_{13} - \boldsymbol{\mu}_{12}) + \left(1-\sqrt{3}\right)(\boldsymbol{\mu}_{13} - \boldsymbol{\mu}_{14})\right], \tag{15g}$$

$$\langle \Psi_4, N+1|\boldsymbol{\mu}|\Psi_4, N\rangle = -\frac{\sqrt{3}}{6}(\boldsymbol{\mu}_{12} + \boldsymbol{\mu}_{13} + \boldsymbol{\mu}_{14}), \tag{15h}$$

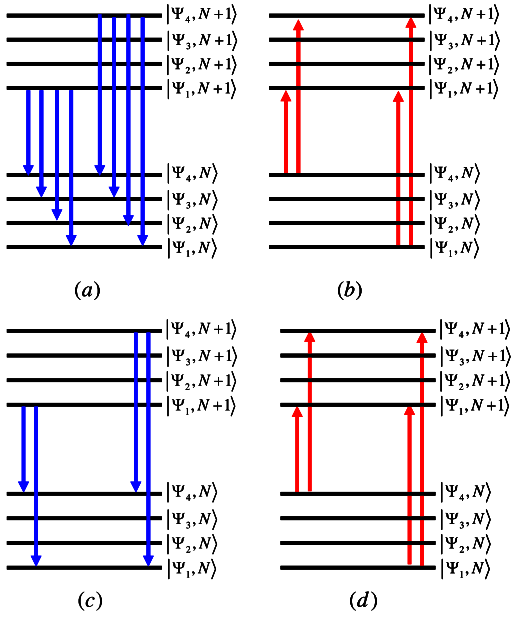

Fig. 2. (Color online) (a),(c) Allowed spontaneous transitions and (b),(d) detected transitions by the probe between dressed states of two neighboring manifolds in the case of the nondegenerate levels. For (a) and (b), $p=0$. For (c) and (d), $p=1$. The parameters are $\Delta_c=0$ and $\Omega_2=\Omega_3=\Omega_4$.

$$\langle\Psi_i,N+1|\boldsymbol{\mu}|\Psi_j,N\rangle=0 \qquad (i=2,3;\ j=1,2,3,4). \tag{15i}$$

Equations (15a)–(15i) indicate the allowed transitions and the dipole moments between the dressed states that can determine qualitatively the peak positions and the widths of the spontaneous emission and absorption spectra. Although we have assumed that the three dipoles of the excited state to the ground states are equal in amplitudes, their directions play an important role in the spontaneous emission and absorption processes. For $0\le p<1$, the dipoles are nonparallel, so $\boldsymbol{\mu}_{12}\neq\boldsymbol{\mu}_{13}\neq\boldsymbol{\mu}_{14}$, and then we have $\langle\Psi_i,N+1|\boldsymbol{\mu}|\Psi_j,N\rangle\neq 0$ $(i=1,4;j=2,3)$; while for $p=1$, the dipoles are parallel to each other (i.e., $\boldsymbol{\mu}_{12}=\boldsymbol{\mu}_{13}=\boldsymbol{\mu}_{14}$), and the quantum interference is maximal, so we have $\langle\Psi_i,N+1|\boldsymbol{\mu}|\Psi_j,N\rangle=0$ $(i=1,4;j=2,3)$. The allowed spontaneous transition for $p=0$ and $p=1$ are shown in Figs. 2(a) and 2(c), respectively.

From Eq. (14), Eq. (13) can be simplified as

$$\begin{aligned}H_p&=\frac{1}{2}\mu E_p[e^{-i\omega_p t}(|1\rangle\langle 2|+|1\rangle\langle 3|+|1\rangle\langle 4|)+\text{H.c.}]\\&=\frac{\sqrt{3}}{3}\mu E_p[e^{-i\omega_p t}(|\Psi_1\rangle-|\Psi_4\rangle)(\langle\Psi_1|+\langle\Psi_4|)+\text{H.c.}].\end{aligned} \tag{16}$$

From Eq. (16) we can see that the probe field can be coupled only to such transitions that the initial states are either Ψ_1 or Ψ_4. Therefore the transitions $|\Psi_i,N+1\rangle\leftrightarrow|\Psi_j,N\rangle$ $(i=1,4;j=2,3)$ cannot be detected by the probe beam, despite the fact that the spontaneous transitions $|\Psi_i,N+1\rangle\leftrightarrow|\Psi_j,N\rangle$ $(i=1,4;j=2,3)$ are allowed for $p=0$. The detected transitions by the probe between dressed states of two neighboring manifolds for $p=0$ and $p=1$ are shown in Figs. 2(b) and 2(d), respectively. So the absorption spectra for both $p=0$ and $p=1$ have the same structure, which are contributed by the transitions $|\Psi_i,N+1\rangle\leftrightarrow|\Psi_j,N\rangle$ $(i,j=1,4)$.

In Fig. 3, we present the absorption (gain) spectra of the weak probe for $p=0$ and $p=1$. It can be found that for the case of degenerate ground levels, the spectrum exhibits a conventional Mollow-like profile [28] for both cases. The only difference is that the amplitude of the spectrum for $p=1$ is larger than that for $p=0$.

It is noted that the conventional Mollow-like absorption spectra around $\Delta_p=0$ and $\Delta_p=\pm 2\sqrt{\kappa_+}$ are originated from transitions $|\Psi_i,N+1\rangle\leftrightarrow|\Psi_j,N\rangle$ $(i,j=1,4)$. When $p=1$ $(\theta=0)$, $|\boldsymbol{\mu}_{12}+\boldsymbol{\mu}_{13}+\boldsymbol{\mu}_{14}|$ has the maximal value. Thus the matrix elements $|\Psi_i,N+1\rangle\leftrightarrow|\Psi_j,N\rangle$ $(i,j=1,4)$ have a maximal value. When p decreases from 1, θ increases from 0, $|\boldsymbol{\mu}_{12}+\boldsymbol{\mu}_{13}+\boldsymbol{\mu}_{14}|$ will decrease, and the values of matrix elements $|\Psi_i,N+1\rangle\leftrightarrow|\Psi_j,N\rangle$ $(i,j=1,4)$ will decrease. As a result, the amplitude of the spectrum will decrease correspondingly, which is shown in Fig. 3.

B. Case of the Nondegenerate Levels

We plot in Fig. 4 the absorption spectra with a nonzero splitting of the three ground levels and different degrees of quantum interference. In Fig. 4(a), one finds that for $p=0$, the spectrum exhibits two dispersionlike lines in the far sidebands (the same as in the degenerate case), between which there are two pairs of gain peaks in the near sidebands. As p increases, the amplitude of the two pairs of gain peaks decreases [shown in Fig. 4(b)]. When the SGC effect is a little less than the maximal value (i.e., $p=0.917$), the two pairs of gain peaks almost disappear [shown in Fig. 4(c)]. When $p=1$, the SGC effect is maximal, and the two pairs of emission peaks evolve into absorption peaks, as seen in Fig. 4(d). From Fig. 4 we can see that the gain spectrum is dramatically affected by the SGC when $\omega\neq 0$.

The preceding features can be understood in terms of the dipole moments between the dressed states and the interaction Hamiltonian described in Section 3. For the nondegenerate case, the dressed states and their eigenvalues as well as the dipole moments between dressed states as expressed by Eqs. (8–12) are still valid. From Eq. (12), we can see that all the dipole matrix elements are nonzero for $\omega\neq 0$. Then the spontaneous emission can occur for all possible transitions $|\Psi_i,N+1\rangle\rightarrow|\Psi_j,N\rangle$ $(i,j=1,2,3,4)$ [shown in Fig. 5(a)], despite the value of p.

In such a case, the interaction Hamiltonian of the probe beam with the atom is determined by Eq. (13). We can calculate that $\sum_{k=2}^{4}C^*_{2(3)k}\ll\sum_{k=2}^{4}C^*_{1(4)k}$, which means that the coupling between the probe field and the atomic dipole mo-

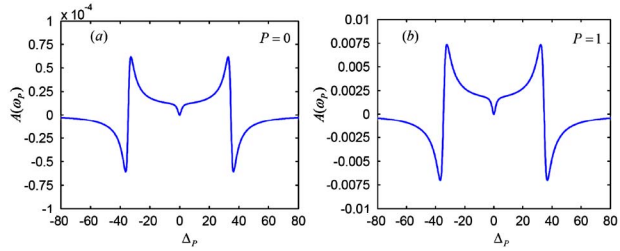

Fig. 3. (Color online) Gain spectra of the weak probe for $\omega_{23}=\omega_{34}=0$. (a) $p=0$, (b) $p=1$. Other parameters are $\gamma_{23}=\gamma_{24}=\gamma_{34}=0.01\gamma$, $\gamma_{12}=\gamma_{13}=\gamma_{14}=\gamma$, $\Delta_c=0$, and $\Omega_2=\Omega_3=\Omega_4=10\gamma$.

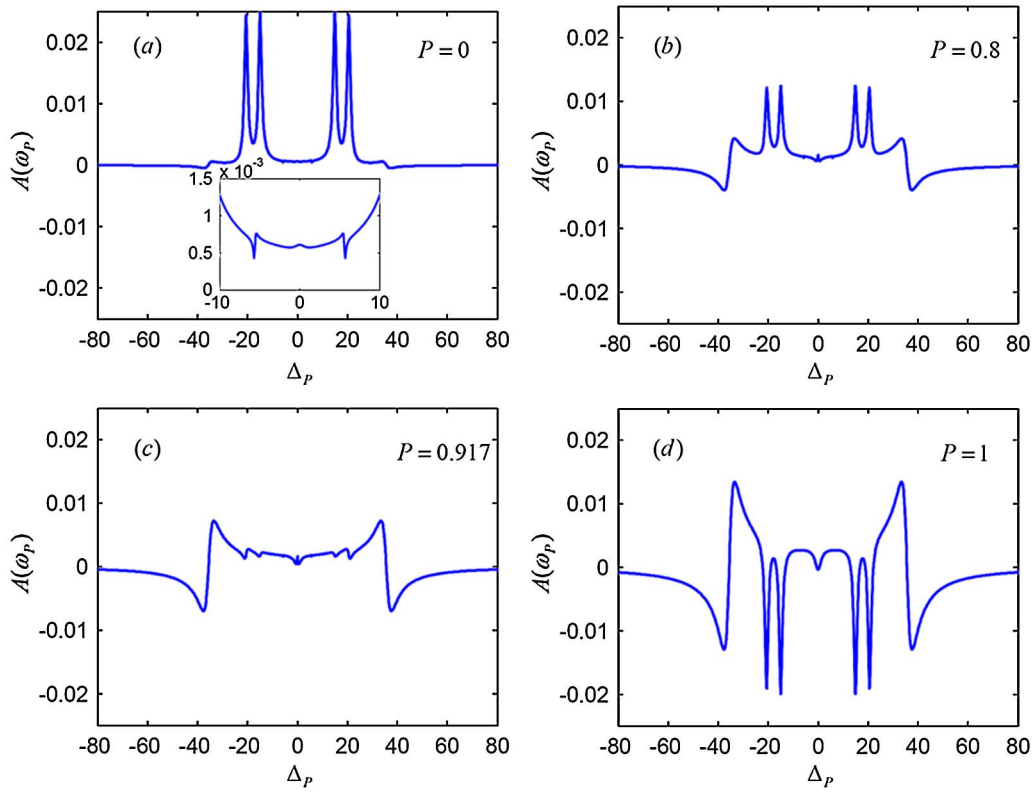

Fig. 4. (Color online) Gain spectra of the weak probe for $\omega_{23} = \omega_{23} = 5\gamma$, with different degrees of SGC: (a) $p = 0$, (b) $p = 0.8$, (c) $p = 0.917$, and (d) $p = 1$. Other parameters are the same as those in Fig. 3.

ment of $|\Psi_i, N+1\rangle \leftrightarrow |\Psi_j, N\rangle$ $(i = 1,2,3,4; j = 2,3)$ is very small. Therefore, the probe field is mainly coupled to such transitions where the initial states are either Ψ_1 or Ψ_4, as shown in Fig. 5(b).

So the origin of the various components of the spectrum in Fig. 4 is clear, the transitions $|\Psi_i, N+1\rangle \leftrightarrow |\Psi_j, N\rangle$ $(i = 2,3; j = 1,4)$ give rise to the two pairs of peaks at $\Delta_p = \pm(\sqrt{\kappa_+} + \sqrt{\kappa_-})$ and $\Delta_p = \pm(\sqrt{\kappa_+} - \sqrt{\kappa_-})$ in the absorption spectrum of the probe, while the conventional Mollow-like absorption spectra around $\Delta_p = 0$ and $\Delta_p = \pm 2\sqrt{\kappa_+}$ are attributed to the transitions $|\Psi_i, N+1\rangle \leftrightarrow |\Psi_j, N\rangle$ $(i, j = 1,4)$. Moreover, it is noted that there are dispersionlike peaks with extremely small amplitudes near the inner gain peaks as shown in the inset of Fig. 4(a), which arises from the transitions $|\Psi_2, N+1\rangle \leftrightarrow |\Psi_3, N\rangle$ and $|\Psi_3, N+1\rangle \leftrightarrow |\Psi_2, N\rangle$. The small amplitude of the absorption peak is attributable to the small coupling between the probe field and the atomic dipole moment of these two transitions.

It is to be noted that the two pairs of gain peaks or absorption peaks depend on the population difference of the states $|\Psi_i, N+1\rangle$ $(i = 2,3)$ and $|\Psi_j, N\rangle$ $(j = 1,4)$. If the population of $|\Psi_i, N+1\rangle$ $(i = 2,3)$ is larger than $|\Psi_j, N\rangle$ $(j = 1,4)$, then the population inversion occurs and we can obtain two pairs of gain peaks. However, when the population of $|\Psi_i, N+1\rangle$ $(i = 2,3)$ is less than $|\Psi_j, N\rangle$ $(j = 1,4)$, the two pairs of peaks turn out to be absorption peaks because there is no inversion in the dressed states. The origin of this striking behavior can be made transparent by the analysis of the population of the dressed states. We plot in Fig. 6 the steady-state population of the dressed states as a function of quantum interference p. It is clearly seen that for values p less than 0.917, the population of states $|\Psi_2\rangle$ and $|\Psi_3\rangle$ (red solid line) is larger than that of states $|\Psi_1\rangle$ and $|\Psi_4\rangle$ (blue dotted line). So the inversion can occur over a wide range of p, and the gain peaks can be obtained. When $p = 0$, the population of states $|\Psi_2\rangle$ and $|\Psi_3\rangle$ is maximal, while the population of states $|\Psi_1\rangle$ and $|\Psi_4\rangle$ is minimal. So the amplitude of the gain peaks has a maximal value [shown in Fig. 4(a)]. When p increases from zero to 0.8, the population of states $|\Psi_2\rangle$ and $|\Psi_3\rangle$ decreases and the population of states $|\Psi_1\rangle$ and $|\Psi_4\rangle$ increases. As a result, the gain peaks decrease correspondingly, as shown in Fig. 4(b). Whereas for values of p close to unity, the population is transferred to the dressed states $|\Psi_1\rangle$ and $|\Psi_4\rangle$. In this case the population inversion vanishes and the absorption peaks turn up [shown in Fig. 4(d)]. Particularly, the population of the states $|\Psi_2\rangle$ and $|\Psi_3\rangle$ and that of $|\Psi_1\rangle$ and $|\Psi_4\rangle$ can be the same when

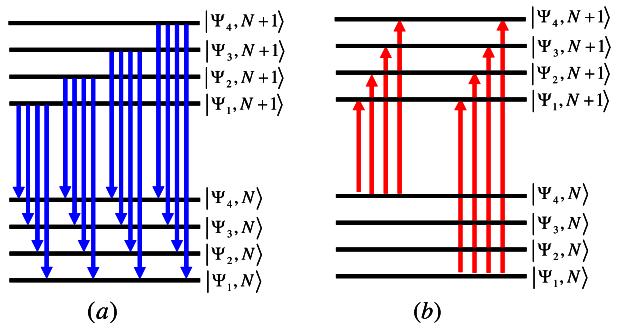

Fig. 5. (Color online) (a) Allowed spontaneous transitions and (b) detected transitions by the probe between dressed states of two neighboring manifolds. (The transitions for $p = 0$ and $p = 1$ are the same.) Other parameters are the same as those in Fig. 2.

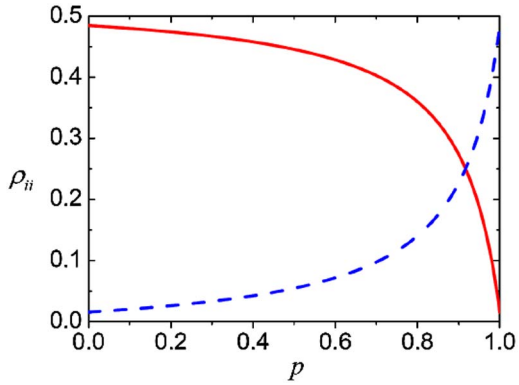

Fig. 6. (Color online) Steady-state population of the dressed states as a function of p. $\rho_{\Psi_1\Psi_1} = \rho_{\Psi_4\Psi_4}$ (blue dotted line); $\rho_{\Psi_2\Psi_2} = \rho_{\Psi_3\Psi_3}$ (red solid line). Parameters are $\omega_{23} = \omega_{34} = 5\gamma$. Other parameters are the same as those in Fig. 2.

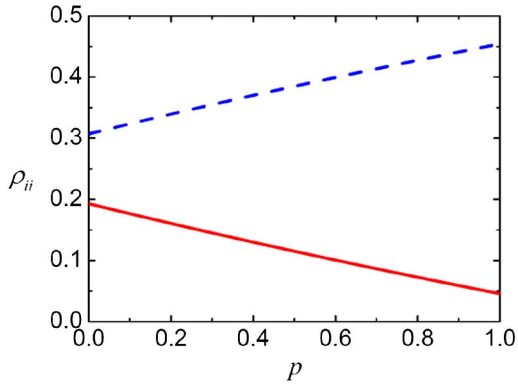

Fig. 7. (Color online) Steady-state population of the dressed states as a function of p. $\rho_{\Psi_1\Psi_1} = \rho_{\Psi_4\Psi_4}$ (blue dotted line); $\rho_{\Psi_2\Psi_2} = \rho_{\Psi_3\Psi_3}$ (red solid line). Parameters are $\omega_{23} = \omega_{34} = 20\gamma$. Other parameters are the same as those in Fig. 2.

$p \approx 0.917$. In this case neither the gain peaks nor the absorption peaks can be obtained [Fig. 4(c)].

As mentioned previously, the transitions $|\Psi_i, N+1\rangle \leftrightarrow |\Psi_j, N\rangle$ $(i = 2,3; j = 1,4)$ are responsible for the peaks at $\Delta_p = \pm(\sqrt{\kappa_+} + \sqrt{\kappa_-})$ and $\Delta_p = \pm(\sqrt{\kappa_+} - \sqrt{\kappa_-})$ in the absorption spectra of the probe. From Eqs. (9)–(12), it can be seen that the magnitude and the position of the gain (or absorption) peaks should be affected by the frequency separation ω. Now let us consider the case of a larger value of ω. We plot in Fig. 7 the steady-state population of the dressed states as a function of p for $\omega = 20$. It can be seen that the population of states $|\Psi_2\rangle$ and $|\Psi_3\rangle$ is less than the population of states $|\Psi_1\rangle$ and $|\Psi_4\rangle$ for all value of p. So it is impossible to obtain population inversion between $|\Psi_i, N+1\rangle$ $(i = 2,3)$ and $|\Psi_j, N\rangle$ $(j = 1,4)$. Thus under the larger value of ω, the transition $|\Psi_i, N+1\rangle (i = 2,3) \leftrightarrow |\Psi_j, N\rangle (j = 1,4)$ corresponds to absorption peaks at $\Delta_p = \pm(\sqrt{\kappa_+} \pm \sqrt{\kappa_-})$. When p increases from 0, the absorption peaks will be enhanced because of the much higher population of states $|\Psi_1\rangle$ and $|\Psi_4\rangle$. And when $p = 1$, we have the maximal population of states $|\Psi_1\rangle$ and $|\Psi_4\rangle$. So the absorption peaks achieve the maximum value. Figure 8 presents the corresponding numerical results for a large value of ω. It can be found that the probe spectra are indeed characterized by two pairs of absorption peaks located at $\Delta_p = \pm(\sqrt{\kappa_+} \pm \sqrt{\kappa_-})$, and the transitions $|\Psi_1, N+1\rangle \leftrightarrow |\Psi_4, N\rangle$ and $|\Psi_4, N+1\rangle \leftrightarrow |\Psi_1, N\rangle$ are responsible for the dispersionlike lines at $\Delta_p = \pm 2\sqrt{\kappa_+}$.

To demonstrate the transition of the gain spectra to absorption spectra as frequency separation changes, we plot the steady-state population of the dressed states as a function of

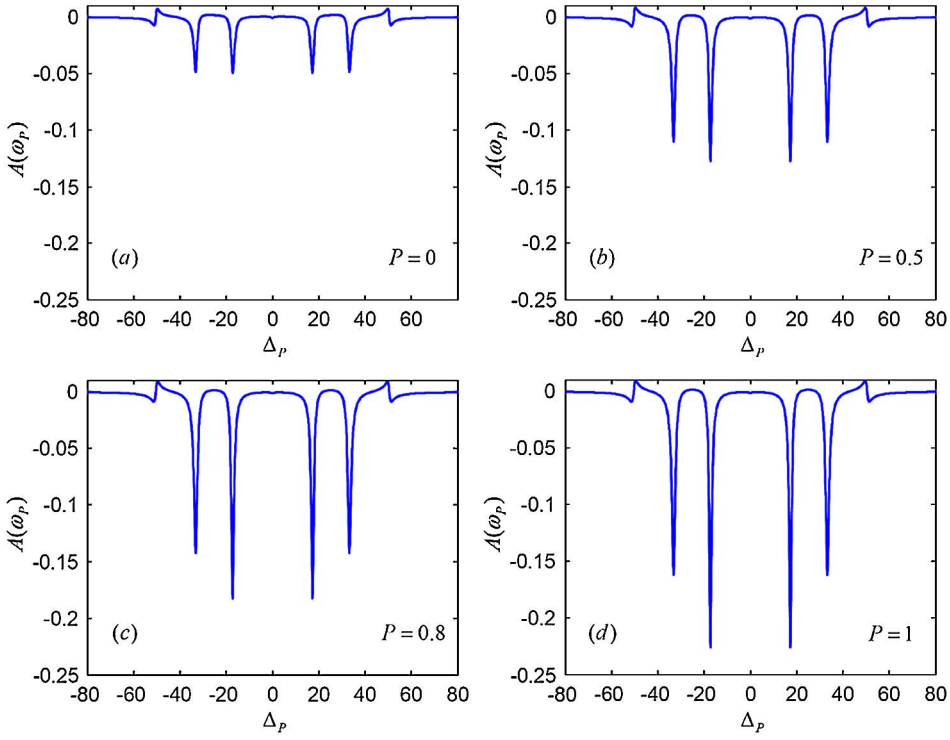

Fig. 8. (Color online) Gain spectra of the weak probe for $\omega_{23} = \omega_{34} = 20\gamma$, with different degrees of the SGC: (a) $p = 0$, (b) $p = 0.5$, (c) $p = 0.8$, and (d) $p = 1$. Other parameters are the same as those in Fig. 3.

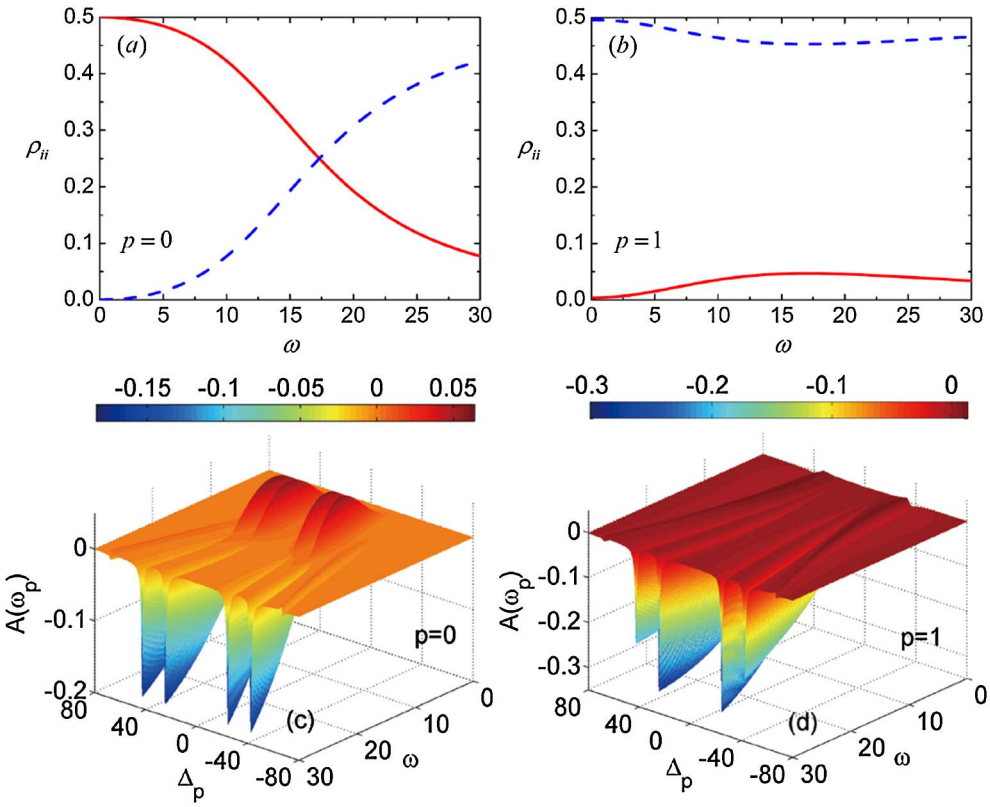

Fig. 9. (Color online) (a),(b) Steady-state populations of the dressed states as a function of ω. $\rho_{\Psi_1\Psi_1} = \rho_{\Psi_4\Psi_4}$ (blue dotted line); $\rho_{\Psi_2\Psi_2} = \rho_{\Psi_3\Psi_3}$ (red solid line). For (a), $p = 0$; for (b), $p = 1$. (c),(d) Probe spectra as functions of frequency separation ω and detuning frequency Δ_p. For (c), $p = 0$; for (d), $p = 1$. Other parameters are the same as those in Fig. 3.

frequency separation ω in Figs. 9(a) and 9(b) and the probe spectra as functions of frequency separation ω and detuning frequency Δ_p in Figs. 9(c) and 9(d) for $p = 0$ and $p = 1$. For $p = 0$, in the case of $\omega = 0$, transitions $|\Psi_i, N+1\rangle \leftrightarrow |\Psi_j, N\rangle$ $(i = 2, 3; j = 1, 4)$ are uncoupled by the probe field [see Eq. (16)]. So there are neither absorption nor gain peaks at $\Delta_p = \pm(\sqrt{\kappa_+} \pm \sqrt{\kappa_-})$. When $\omega \neq 0$, from Eq. (13) we can see that transitions $|\Psi_i, N+1\rangle \leftrightarrow |\Psi_j, N\rangle$ $(i = 2, 3; j = 1, 4)$ can be probed. As can be seen from Fig. 9(a), when ω is small, the population of the dressed states $|\Psi_2\rangle$ and $|\Psi_3\rangle$ is larger than that of $|\Psi_1\rangle$ and $|\Psi_4\rangle$. So there are two pairs of gain peaks. As ω is increased, $\rho_{\Psi_2\Psi_2}(\rho_{\Psi_3\Psi_3})$ is decreased while $\rho_{\Psi_1\Psi_1}(\rho_{\Psi_4\Psi_4})$ is increased. Eventually $\rho_{\Psi_2\Psi_2}(\rho_{\Psi_3\Psi_3}) < \rho_{\Psi_1\Psi_1}(\rho_{\Psi_4\Psi_4})$ and gain peaks turn out to be absorption peaks. This variation is shown in Fig. 9(c). For $p = 1$, it can be seen from Fig. 9(b) that $\rho_{\Psi_2\Psi_2}(\rho_{\Psi_3\Psi_3}) < \rho_{\Psi_1\Psi_1}(\rho_{\Psi_4\Psi_4})$. Thus it is impossible to realize population inversion between $|\Psi_i, N+1\rangle$ $(i = 2, 3)$ and $|\Psi_j, N\rangle$ $(j = 1, 4)$. As a result there are always absorption peaks in the spectra [see Fig. 9(d)].

5. POSSIBLE EXPERIMENTS

To observe the predicted phenomena associated with SGC, we need three closely separated levels with nonorthogonal dipole moments. It is worth noting that so far no real atoms or molecules have been found to exhibit observable SGC owing to the rigorous conditions of nearly degenerate levels and nonorthogonal dipole moments. Fortunately the tripod-type atom can be attained in a four-level N-type system without SGC, which is equivalent to a four-level tripod-type atom with SGC in the dressed-state representation of two additional coupling fields ω_1 and ω_2. The transition dipoles of the three dressed states to the excited level would be parallel, which satisfies the specific arrangement on dipole moments and field polarizations in the four-level tripod-type system [see Fig. 10].

To be more specific for potential experiments, we point out that a four-level N-type system can be found in the Rb atoms. A cold atomic system [30,31] or the atomic beam [18–20] should be used to avoid Doppler broadening. The coupling laser ω_1 and ω_2 drive $D_1F = 2 \rightarrow F' = 1$ and $D_1F = 1 \rightarrow F' = 1$ transition at 795 nm. The other laser ω drives the $D_2F = 2 \rightarrow F' = 3$ transition at 780 nm and a weak probe laser ω_p probes the same transition. By applying the two coupling lasers ω_1 and ω_2, the system is equivalent to a four-level tripod-type atom with SGC in the dressed-state representation, in which

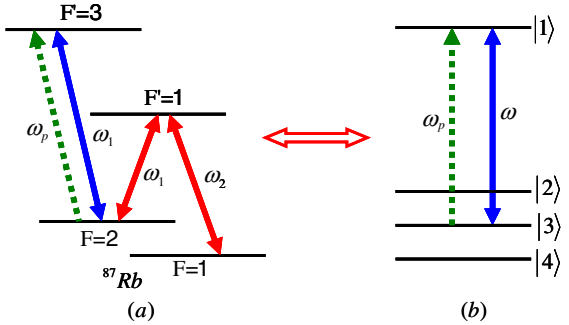

Fig. 10. (Color online) (a) Four-level N-type system without SGC; (b) four-level tripod-type atomic system with SGC. The former one is equivalent to the latter one in the dressed-state representation of two additional fields ω_1 and ω_2.

both the coupling laser ω and probe laser ω_p interact simultaneously with three different transitions. It can be expected that the experimental demonstration of various effects of the SGC on the radiative properties of the atomic systems should be possible.

6. CONCLUSION

In summary, we have investigated the gain spectra for a weak probe in a tripod-type atom with SGC, where a single laser field drives all transitions from the upper state to the lower states simultaneously. We studied the distinct cases of the degenerate and nondegenerate ground levels. It is pointed out that the gain spectra can be explained by introducing dipole moments and the Hamiltonian in terms of dressed states. For the degenerate case, the gain spectrum exhibits a conventional Mollow-like profile, and the SGC influence only the amplitudes of the absorption (gain) peaks without affecting the spectrum structure. And this can be understood by the fact that two of the four dressed states have zero population and do not contribute to the gain process. While in the nondegenerate case, the gain spectra not only are strongly dependent on the effect of SGC but also are dependent on the energy separation of the three closely lying ground levels. When the separation is not large, the amplitudes of the gain peaks are influenced by the SGC factor p because the variation of p can modify the population of the dressed states. In the absence of quantum interference, the spectrum may exhibit two pairs of gain peaks in the near sidebands, which is caused by population inversion in the dressed states. When quantum interference is maximal, the two pairs of gain peaks evolve into absorption peaks, which is unlike the case in [27]. This is because all the matrix elements of the atomic dipole moment in the dressed-state picture are nonzero and the population inversion in the dressed states is not achieved. In the case of larger energy separation of the ground levels, the spectrum exhibits two pairs of absorption peaks in the near sidebands even when $p = 0$ because under this condition population inversion between dressed states cannot be achieved. When p increases from 0 to 1, the absorption peaks will be enhanced because of the larger population difference in the dressed states. Finally, we discuss a possible experiment to attain these results. The experimental suggestion is applying two coherent fields on three of the four levels in an N-type four-level system without SGC.

ACKNOWLEDGMENTS

The authors would like to thank the National Basic Research Program (Grant No. 2011CB921603) of P. R. China and NSFC (Grants No. 11074097, No. 10904048, No. 10974071, and No. 11004080) for support.

REFERENCES

1. G. J. Yang, M. Xie, Z. Zhang, and K. Wang, "Effect of vacuum-induced coherences on coherent population trapping of moving atoms," Phys. Rev. A **77**, 063825 (2008).
2. X. H. Yang and S. Y. Zhu, "Control of coherent population transfer via spontaneous decay-induced coherence," Phys. Rev. A **77**, 063822 (2008).
3. E. Paspalakis, N. J. Kylstra, and P. L. Knight, "Transparency induced via decay interference," Phys. Rev. Lett. **82**, 2079–2082 (1999).
4. E. Paspalakis, N. J. Kylstra, and P. L. Knight, "Transparency of a short laser pulse via decay interference in a closed V-type system," Phys. Rev. A **61**, 045802 (2000).
5. M. A. Antón, Oscar G. Calderón, and F. Carreño, "Spontaneously generated coherence effects in a laser-driven four-level atomic system," Phys. Rev. A **72**, 023809 (2005).
6. A. Fountoulakis, A. F. Terzis, and E. Paspalakis, "Coherent phenomena due to double-dark states in a system with decay interference," Phys. Rev. A **73**, 033811 (2006).
7. C. H. Raymond Ooi, "Effects of spontaneously generated coherence on two-photon correlation in a double-cascade scheme," Phys. Rev. A **75**, 043818 (2007).
8. J. W. Gao, Q. Q. Bao, R. G. Wan, C. L. Cui, and J. H. Wu, "Triple photonic band-gap structure dynamically induced in the presence of spontaneously generated coherence," Phys. Rev. A **83**, 053815 (2011).
9. Y. P. Yang, J. P. Xu, H. Chen, and S. Y. Zhu, "Quantum interference enhancement with left-handed materials," Phys. Rev. Lett. **100**, 043601 (2008).
10. V. Yannopapas, E. Paspalakis, and N. V. Vitanov, "Plasmon-induced enhancement of quantum interference near metallic nanostructures," Phys. Rev. Lett. **103**, 063602 (2009).
11. G. S. Agarwal, "Anisotropic vacuum-induced interference in decay channels," Phys. Rev. Lett. **84**, 5500–5503 (2000).
12. Z. Ficek and S. Swain, "Simulating quantum interference in a three-level system with perpendicular transition dipole moments," Phys. Rev. A **69**, 023401 (2004).
13. J. H. Wu, A. J. Li, Yue Ding, Y. C. Zhao, and J. Y. Gao, "Control of spontaneous emission from a coherently driven four-level atom," Phys. Rev. A **72**, 023802 (2005).
14. A. J. Li, J. Y. Gao, J. H. Wu, and Lei Wang, "Simulating spontaneously generated coherence in a four-level atomic system," J. Phys. B **38**, 3815–3823 (2005).
15. J. H. Li, J. B. Liu, A. X. Chen, and C. C. Qi, "Spontaneous emission spectra and simulating multiple spontaneous generation coherence in a five-level atomic medium," Phys. Rev. A **74**, 033816 (2006).
16. A. J. Li, X. L. Song, X. G. Wei, L. Wang, and J. Y. Gao, "Effects of spontaneously generated coherence in a microwave-driven four-level atomic system," Phys. Rev. A **77**, 053806 (2008).
17. Z. H. Li, D. W. Wang, H. Zheng, S. Y. Zhu, and M. S. Zubairy, "Quantum interference due to energy shifts and its effect on spontaneous emission," Phys. Rev. A **82**, 050501(R)(2010).
18. C. L. Wang, A. J. Li, X. Y. Zhou, Z. H. Kang, Y. Jiang, and J. Y. Gao, "Investigation of spontaneously generated coherence in dressed states of 85Rb atoms," Opt. Lett. **33**, 687–689 (2008).
19. C. L. Wang, Z. H. Kang, S. C. Tian, Y. Jiang, and J. Y. Gao, "Effect of spontaneously generated coherence on absorption in a V-type system: investigation in dressed states," Phys. Rev. A **79**, 043810 (2009).
20. S. C. Tian, Z. H. Kang, C. L. Wang, R. G. Wan, J. Kou, H. Zhang, Y. Jiang, H. N. Cui, and J. Y. Gao, "Observation of spontaneously generated coherence on absorption in rubidium atomic beam," Opt. Commun. **285**, 294–299 (2012).
21. P. Zhou and S. Swain, "Quantum interference in probe absorption: narrow resonances, transparency, and gain without population inversion," Phys. Rev. Lett. **78**, 832–835 (1997).
22. S. Menon and G. S. Agarwal, "Gain components in the Autler-Townes doublet from quantum interferences in decay channels," Phys. Rev. A **61**, 013807 (1999).
23. P. Dong and S. H. Tang, "Absorption spectrum of a V-type three-level atom driven by a coherent field," Phys. Rev. A **65**, 033816 (2002).
24. S. Menon and G. S. Agarwal, "Effects of spontaneously generated coherence on the pump-probe response of a Λ system," Phys. Rev. A **57**, 4014–4018 (1998).
25. W. H. Xu, J. H. Wu, and J. Y. Gao, "Effects of spontaneously generated coherence on transient process in a Λ system," Phys. Rev. A **66**, 063812 (2002).
26. J. H. Wu and J. Y. Gao, "Phase control of light amplification without inversion in a Λ system with spontaneously generated coherence," Phys. Rev. A **65**, 063807 (2002).
27. W. H. Xu and J. Y. Gao, "Gain spectrum of a laser-driven-type atom with vacuum-induced coherence," J. Opt. Soc. Am. B **22**, 2385–2392 (2005).

28. B. R. Mollow, "Stimulated emission and absorption near resonance for driven systems," Phys. Rev. A **5**, 2217–2222 (1972).
29. L. M. Narducci, M. O. Scully, G. L. Oppo, P. Ru, and J. R. Tredicce, "Spontaneous emission and absorption properties of a driven three-level system," Phys. Rev. A **42**, 1630–1649 (1990).
30. M. Yan, E. G. Rickey, and Y. F. Zhu, "Observation of doubly dressed states in cold atoms," Phys. Rev. A **64**, 013412 (2001).
31. H. Kang, G. Hernandez, and Y. F. Zhu, "Superluminal and slow light propagation in cold atoms," Phys. Rev. A **70**, 011801(R) (2004).